Crossed-Beam and Theoretical Studies of the $S(^1D) + C_2H_2$ Reaction†

Francesca Leonori, Raffaele Petrucci, Nadia Balucani, Kevin M. Hickson,‡ Mathias Hamberg,§ Wolf D. Geppert,§ and Piergiorgio Casavecchia*

Dipartimento di Chimica, Università degli Studi di Perugia, 06123 Perugia, Italy

Marzio Rosi

Dipartimento di Ingegneria Civile e Ambientale and ISTM-CNR, c/o Dipartimento di Chimica, Università degli Studi di Perugia, 06123 Perugia, Italy

Received: December 12, 2008; Revised Manuscript Received: January 31, 2009

The reaction dynamics of excited sulfur atoms, $S(^1D)$, with acetylene has been investigated by the crossed-beam scattering technique with mass spectrometric detection and time-of-flight (TOF) analysis at the collision energy of 35.6 kJ mol^{-1}. These studies have been made possible by the development of intense continuous supersonic beams of $S(^3P,^1D)$ atoms. From product angular and TOF distributions, center-of-mass product angular and translational energy distributions are derived. The $S(^1D) + C_2H_2$ reaction is found to lead to formation of HCCS (thioketenyl) + H, while the only other energetically allowed channels, those leading to $CCS(^3\Sigma^-, ^1\Delta) + H_2$, are not observed to occur to an appreciable extent. The dynamics of the H-elimination channel is discussed and elucidated. The interpretation of the scattering results is assisted by synergic high-level ab initio electronic structure calculations of stationary points and product energetics for the C_2H_2S ground-state singlet potential energy surface. In addition, by exploiting the novel capability of performing product detection by means of a tunable electron-impact ionizer, we have obtained the first experimental information on the ionization energy of thioketenyl radical, HCCS, as synthesized in the reactive scattering experiment. This has been complemented by ab initio calculations of the adiabatic and vertical ionization energies for the ground-state radical. The theoretically derived value of 9.1 eV confirms very recent, accurate calculations and is corroborated by the experimentally determined ionization threshold of 8.9 ± 0.3 eV for the internally warm HCCS produced from the title reaction.

1. Introduction

The chemical reactivity of atomic sulfur with inorganic and organic molecules is an intriguing subject of research, but as yet, mostly unexplored. A motivation to initiate an experimental study of the elementary reactions of sulfur atoms resides in their potential role in many different areas, such as material sciences (especially in the production of sulfur-doped diamond[1−3]), combustion of S-containing fuel and coal,[4] atmospheric chemistry,[5] and astrochemistry.[6−9] Sulfur oxidation and the formation of sulfur oxides is certainly the topic of major concern in the evaluation of the environmental impact of sulfur and its compounds because of the well-known problem of acid rain. Nevertheless, some interesting processes also involve the reduced forms of sulfur, as witnessed by the identification of simple molecules or radicals containing a C−S bond during the combustion of sulfur-rich fossil fuels.[4] Similar species have been identified[1] during the chemical vapor deposition of sulfur-doped diamond starting from CH_4/H_2S mixtures. Remarkably, it has been demonstrated that the combustion of sulfur-rich fossil fuels produces more soot than the sulfur-poor ones,[10] while the formation of the CS radical in the gas-phase has been suggested to be the first step toward sulfur incorporation into diamond.[2] The addition of small amounts of H_2S into the gas used in the deposition of diamond has also been seen to influence the morphology of the diamond crystals.[2,3] All these observations imply that an active form of sulfur, such as atomic sulfur or diatomic sulfur S_2, directly interacts with the relevant hydrocarbons or hydrocarbon radicals, thus affecting the final outcome of these processes to some extent. The observation of simple organo-sulfur compounds in other environments (such as in the interstellar medium[6,7] and cometary comae[8]) also poses the question of how they are formed in such different conditions. Among those observations, probably the most striking one is the detection of CS, CS_2, and S_2 after the impact of the comet Shoemaker-Levy 9 on Jupiter, where those species were observed after the impact for several days.[11] Some possible mechanisms of C−S bond formation were suggested[12] and several were investigated in crossed beam experiments.[13,14]

As a matter of fact, it is the substantial lack of experimental data, both at the level of kinetic investigation and of reaction dynamics, that has prevented us from establishing the actual role of the reactions of atomic sulfur with hydrocarbons or hydrocarbon radicals in all of the above-mentioned processes. To this end, in our laboratory we have started a systematic investigation of atomic sulfur reactions by means of the crossed molecular beam (CMB) technique with mass-spectrometric (MS) detection. Our investigations exploit the novel capability of generating intense continuous supersonic beams of sulfur atoms from a radio frequency (rf) discharge beam source, similar in design to that described by Sibener et al.[15] for oxygen atom

† Part of the "George C. Schatz Festschrift".

* To whom correspondence should be addressed. E-mail: piero@dyn.unipg.it. Tel.: +39 075 585 5514. Fax: +39 075 585 5606.

‡ Present address: Institut des Sciences Moléculaires, Université Bordeaux 1, 33405 Talence Cedex, France.

§ Permanent address: Molecular Physics Division, Department of Physics, Alba Nova, University of Stockholm, S-10691 Stockholm, Sweden.

10.1021/jp810989p CCC: $40.75
Published on Web 03/04/2009

beam production, and which has been successfully used in our laboratory to produce other atomic and molecular radical beams.[16−21] For the production of atomic sulfur we have chosen SO_2 as molecular precursor and, similarly to the case of the production of beams of atomic oxygen and carbon,[19,20,22−24] we have obtained experimental evidence that the sulfur atoms are produced not only in the ground electronic state, ^{3}P, but also in the first electronically excited, metastable state ^{1}D. As in previous cases,[19,20,22,23] the presence of both species in the beam allows us either to investigate the reactions of S(^{1}D) when the ^{3}P state is not reactive or the reactivity of both species when both react. In the latter case, by performing high resolution experiments we can separate the two contributions because of the different energetics and, possibly, dynamics, as previously done for O(^{3}P,^{1}D) and C(^{3}P,^{1}D).[19,20] Noticeably, the only previous reaction dynamics studies of S-atoms were carried out on two reactions of S(^{1}D); Liu and co-workers have investigated the reaction S(^{1}D) + H_2 (and isotopic variants) by using a pulsed CMB apparatus with laser photolysis generation of S atoms and REMPI detection of the H product within a Doppler-shift scheme,[25] while Dagdigian and co-workers performed LIF studies of the SD product rotational distribution from the S(^{1}D) + D_2 and S(^{1}D) + CD_4 reactions[26,27] in a photolysis-probe experiment in a low-pressure quasi-static cell. In general, the reactions of S(^{1}D) may also be of considerable relevance, especially in atmospheric chemistry. In fact, several reduced sulfur compounds (such as CH_3SCH_3, CS_2, CH_3SH, CH_3SSCH_3, H_2S, and OCS) are abundantly released at the earth surface from biogenic sources. Some of these species might survive and enter the stratosphere or be injected directly into the stratosphere by volcanic eruption.[28] In the upper part of the atmosphere, those sulfur compounds undergo UV photodissociation. For instance, OCS can be photodissociated in the window between the O_2 and O_3 absorptions producing CO and S(^{3}P,^{1}D) and it is agreed that the spin-allowed production of S(^{1}D) is the dominant process.[29] Even the photodissociation of H_2S at the Lyman-α wavelength can occur via a three body dissociation with S(^{1}D) formation.[30] Since the lifetime of the metastable excited-state is long enough (28 s),[31] sulfur atoms in the excited ^{1}D state may well react with atmospheric constituents. The rate coefficients for S(^{1}D) removal from several species at 300 K have been measured and compared with those of the related species O(^{1}D)[32] of great relevance in atmospheric chemistry. The rate coefficients are very fast and similar in the two cases. In addition to that, S(^{1}D) might be produced in the dissociation of H_2S in the chemical vapor deposition processes that exploits plasma production by microwave or radiofrequency discharge. It should be noted that in those processes a significant portion of methane is rapidly converted to acetylene.[1,2]

In this paper, we present the first report of crossed beam experiments on the reaction of atomic sulfur with hydrocarbons. Specifically, the reaction that is the subject of the present work is the one between atomic sulfur in the first electronically excited-state with a simple unsaturated hydrocarbon, namely acetylene. In contrast to the analogous reaction involving O(^{3}P) and C(^{3}P), sulfur atoms in the ground ^{3}P state do not react with acetylene, as recently pointed out by ab initio calculations that have derived a large endothermicity for the only possible reactive channel leading to HCCS + H (ΔH_0° = +84.8 kJ mol^{-1}).[33] The theoretical results give an indication that contrasts with old results of kinetic experiments. Little and Donovan measured the absolute rate for the S(^{3}P) removal by C_2H_2 (at 295 K) to be $5.0 \pm 0.5 \times 10^{-13}$ cm^3 molecule^{-1} s^{-1} using flash photolysis with time-resolved atomic absorption in the vacuum UV.[34] Using a similar technique, Gunning and co-workers performed a detailed investigation of S(^{3}P) reactions with a series of alkynes, including acetylene.[35] An activation energy of ∼12 kJ mol^{-1} was inferred for the S(^{3}P) + C_2H_2 reaction,[35] but such a small activation barrier is clearly not in line with the large endothermicity of the only possible reactive channel. The reaction of S(^{1}D) with acetylene was also investigated by kinetic experiments and found to be much faster with a room temperature rate constant of $\sim 5.0 \times 10^{-11}$ cm^3 molecule^{-1} s^{-1}.[34] In this case, because of the large energy content of the electronically excited state, the H-displacement channel is exothermic and amenable to the reactive system.

The possible reaction channels are

$$S(^1D) + C_2H_2 \rightarrow HCCS(^2\Pi) + H(^2S) \qquad \Delta H_0^\circ = -36.0 \text{ kJ mol}^{-1} \quad (1)$$

$$\rightarrow HSCC(^2A'') + H(^2S) \qquad \Delta H_0^\circ = +162.4 \text{ kJ mol}^{-1} \quad (2)$$

$$\rightarrow c\text{-}HC(S)C(^2A'') + H(^2S) \qquad \Delta H_0^\circ = +84.3 \text{ kJ mol}^{-1} \quad (3)$$

$$\rightarrow CCS(^1\Delta) + H_2 \qquad \Delta H_0^\circ = +27.3 \text{ kJ mol}^{-1} \quad (4)$$

$$\rightarrow CCS(^3\Sigma^-) + H_2 \qquad \Delta H_0^\circ = -30.2 \text{ kJ mol}^{-1} \quad (5)$$

$$\rightarrow CS(^1\Sigma^+) + CH_2(^1A_1) \qquad \Delta H_0^\circ = +92.9 \text{ kJ mol}^{-1} \quad (6)$$

$$\rightarrow CS(^1\Sigma^+) + CH_2(^3B_1) \qquad \Delta H_0^\circ = +54.3 \text{ kJ mol}^{-1} \quad (7)$$

The production of three isomers with general formula C_2HS can be associated to the H-displacement mechanism, but among them only the one leading to HCCS is exothermic. Molecular hydrogen elimination can form either CCS in a singlet state through a quite endothermic channel (4) or CCS in its ground $^3\Sigma^-$ electronic state (5). In this latter case an intersystem crossing (ISC) to the triplet C_2H_2S potential energy surface (PES) is necessary. All the other channels are strongly endothermic. We have experimentally explored the possibility of both H-displacement and H_2-elimination occurrence and complemented the crossed beam results with theoretical calculations of the C_2H_2S singlet PES at the B3LYP and CCSD(T) levels of theory with thermochemical calculations also performed at the W1 level. The enthalpies of reactions reported above are those calculated in the present work. The H_2 elimination channel has not been observed to occur to an appreciable extent under the experimental conditions of our experiments, while the dynamics of the H-displacement channel has been characterized. In addition, by exploiting the recently implemented novel capability[36−38] of measuring electron ionization efficiency curves of reactants as well as reaction products synthesized in CMB experiments, from 100 eV down to very low values (ca. 7 eV), we have investigated both experimentally and theoretically the ionization energy of the thioketenyl (HCCS) radical product, for which no experimental information was available prior to the present study (see Section 7).

2. Experimental Section

We performed scattering experiments at a collision energy, E_c, of 35.6 kJ mol^{-1} using a universal crossed molecular beam apparatus which has been described elsewhere.[17,38] Briefly, two well-collimated, in angle and velocity, continuous supersonic beams of the reactants are crossed at 90° in a large scattering chamber maintained at a pressure of 2×10^{-6} mbar in operating conditions (2×10^{-7} mbar base pressure). The angular and velocity distributions of the products are measured by a rotatable quadrupole mass spectrometer detector equipped with a tunable electron-impact ionizer. The whole detector unit is contained in an ultrahigh-vacuum (10^{-11} mbar) chamber. Continuous supersonic beams of S atoms are generated from a high-pressure, high-power radio frequency (rf) discharge beam source described in ref.[16] By discharging 65 mbar of a 1% SO_2 in helium gas mixture through a 0.55 mm diameter quartz nozzle at 300 W of nominal rf power, a supersonic beam with a peak velocity of 2067 m s^{-1} and a speed ratio of 5.7 was obtained. The characterization of the sulfur beam composition has not been performed yet, but we anticipate that atomic sulfur is mainly produced in the ground ^{3}P state. However, a significant percentage of atomic sulfur in the excited ^{1}D state (lying 110.5 kJ mol^{-1} above the ground state) is also produced and survives during the supersonic expansion, as demonstrated by the present CMB study and others on the S(^{1}D) + CH_4 and S(^{1}D) + C_2H_4 reactions.[39,40] Some S_2 can be present in the beam (not observable directly with the mass-spectrometer because of the presence of some undissociated SO_2 at the same m/z), but none of the reactive experiments we have performed up to now (including the reactions with methane[40] and ethylene[39]) have pointed to a significant presence of this species in the beams.

A supersonic beam of acetylene was generated by expanding 450 mbar of C_2H_2 through a 100 μm diameter stainless-steel nozzle kept at room temperature. The beam peak velocity was 833 m s^{-1} and the speed ratio 5.1. Under these expansion conditions C_2H_2 clustering was negligible. Because of the significant cooling during supersonic expansion, the acetylene molecules in the beam are expected to be in the lowest rotational states of essentially the ground vibrational level, and therefore the internal energy of the molecular reactant contributes negligibly to the total available energy.

The product laboratory angular distributions, N(Θ), were recorded at m/z = 57 (C_2HS^+) and 56 (C_2S^+) by counting for 50 s at each angle and averaging over at least five scans. The C_2H_2 beam was modulated at 160 Hz by a tuning-fork chopper for background subtraction. Velocity analysis of the beams was carried out by conventional "single-shot" time-of-flight (TOF) techniques, using a high-speed multichannel scaler and a CAMAC data acquisition system controlled by a personal computer. Velocity distributions of the products were obtained at ten different angles using the cross-correlation TOF technique with four 127-bit pseudorandom sequences. High-time resolution was achieved by spinning the TOF disk, located at the entrance of the detector, at 393.7 Hz corresponding to a dwell time of 5 μs/channel. The flight length was 24.3 cm. Counting times varied from 20 to 60 min depending upon the signal intensity.

As already mentioned, our crossed beam apparatus features a tunable electron impact ionizer (with an electron energy spanning a range from 100 eV down to ca. 7 eV) to ionize the neutral product species. The use of a tunable ionizer allows us to measure the product electron ionization (EI) efficiency curves as a function of electron energy down to ionization thresholds and, from these, to obtain a direct estimate of the ionization energy of the radical products. In other words, as already pointed out,[36−38] we have developed the capability of deriving the ionization energy (IE) of radical species by "synthesizing" them in CMB reactive scattering experiments. This approach has been applied here to the case of the radical product HCCS for which no previous experimental information on the ionization energy was available.

3. Computational Details

The potential energy surface of the S(^{1}D) + C_2H_2 system was investigated by locating the lowest stationary points at the B3LYP[41] level of theory in conjunction with the correlation consistent valence polarized set aug-cc-pVTZ,[42] augmented with a tight d function with exponent 2.457 for the sulfur atoms[43] to correct for the core polarization effects.[44] This basis set will be denoted aug-cc-pV(T+d)Z. At the same level of theory we have computed the harmonic vibrational frequencies in order to check the nature of the stationary points, that is, minimum if all the frequencies are real, saddle point if there is one, and only one, imaginary frequency. The energy of all the stationary points was computed at the higher level of calculation CCSD(T)[45] using the same basis set aug-cc-pV(T+d)Z. Both the B3LYP and the CCSD(T) energies were corrected to 0 K by adding the zero-point energy correction computed using the scaled harmonic vibrational frequencies evaluated at B3LYP/aug-cc-pV(T+d)Z level. The energy of S(^{1}D) was estimated by adding the experimental[46] separation S(^{3}P) − S(^{1}D) of 110.5 kJ mol^{-1} to the energy of S(^{3}P) at all levels of calculation. Thermochemical calculations were performed at the W1 level of theory.[47] It should be recalled that in the W1 method[47] the geometry optimization and the evaluation of the frequencies are performed at the B3LYP/VTZ + d level while the energies are computed at the CCSD(T)/AVDZ + 2d, CCSD(T)/AVTZ + 2d1f, CCSD/AVQZ + 2d1f level of theory (AVnZ is for aug-cc-pVnZ with n = D, T, Q). All calculations were performed using Gaussian 03[48] while the analysis of the vibrational frequencies was performed using Molekel.[49]

4. Results and Analysis of Reactive Scattering Experiments

In Figure 1 are shown the product laboratory (LAB) angular distributions detected at m/z = 57 (corresponding to the ion C_2HS^+, open circles) and 56 (corresponding to the ion C_2S^+, solid circles) together with the relevant velocity vector ("Newton") diagram. The error bars (representing ±1 standard deviation) are also reported when they exceed the size of the dots indicating the intensity averaged over the different scans. In Figure 2 are shown the m/z = 57, 56 TOF spectra measured at the angle Θ = 19.25°. The measurements at m/z = 56 have been performed in order to verify if the channels (4) or (5) are open under the present experimental conditions. It is to be noted that the ion C_2S^+ can also be formed by the dissociative ionization of the HCCS product (channel 1) in the electron impact ionizer. It can be clearly seen that both LAB angular and TOF distributions recorded at m/z = 56 were found to be fully superimposable on the ones recorded at m/z = 57. This implies that the signal observed at m/z = 56 mostly comes from the dissociative ionization of HCCS product and the channels (4)/(5) give a negligible contribution (if any) to the observed signal. Some reactive signal of smaller intensity was also observed at m/z = 59 and 58 associated with the same product with the mass 34 isotope of sulfur.

All the final measurements were performed at m/z = 57, because of the higher signal-to-noise ratio. TOF spectra at m/z = 57 were measured at ten selected LAB angles. They are

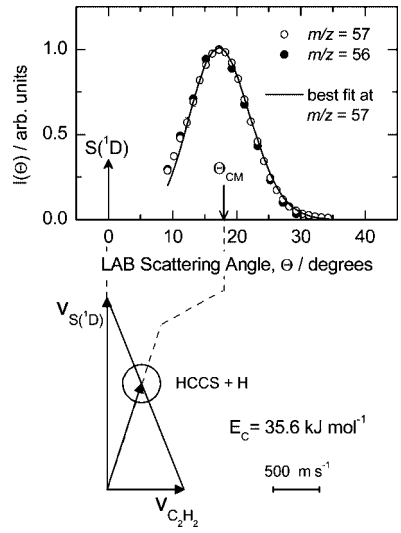

Figure 1. Laboratory angular distributions recorded at $m/z = 57$ (open circles) and $m/z = 56$ (solid circles) for the reaction S(^{1}D) + C_2H_2 at $E_c = 35.6$ kJ mol^{-1}. Error bars, when visible outside the dots, represent ± 1 standard deviation from the mean. The solid line is the total angular distribution calculated when using the best-fit functions reported in Figure 4. The velocity vector (Newton) diagram of the experiment is also shown. The circle in the Newton diagram delimits the maximum velocity that the HCCS product can attain in the CM system on the basis of linear momentum and energy conservation if all the available energy goes into product translational energy.

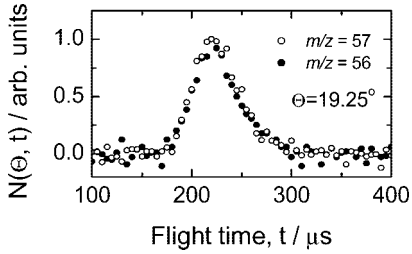

Figure 2. TOF distributions of $m/z = 57$ (open circles) and $m/z = 56$ (solid circles) for the reaction S(^{1}D) + C_2H_2 at $E_c = 35.6$ kJ mol^{-1} at the scattering angle of 19.25° (counting times are 5 and 10 min for the spectra recorded at $m/z = 57$ and 56, respectively).

reported in Figure 3. At the maximum of the angular distribution ($\Theta = 17°$), the signal is about 800 counts/s (emission current = 2 mA; ionizing electron energy = 60 eV) and the signal-to-noise ratio is about 120. The LAB angular distribution is relatively narrow and extends only over 20° in the scattering plane. This is a direct consequence of the experimental kinematics; the combination of masses associated to the formation of a heavy product (HCCS vs H) and the relatively small exothermicity of channel (1) give rise to a small Newton circle (see Figure 1, lower panel) within which HCCS can be scattered. The relatively sharp peak of the LAB angular distribution in the proximity of the center-of-mass angle ($\Theta_{CM} = 18°$) suggests also that the fraction of total available energy released into product translational energy is relatively small. The recorded TOF spectra are also sharp and centered around the CM velocity (see Figure 3).

The scattering measurements are carried out in the LAB system of coordinates, while for the physical interpretation of the scattering process it is necessary to transform the data (angular, N(Θ), and velocity, N(Θ,v) distributions) to a coordinate system which moves with the center-of-mass (CM) of the colliding system. Because of the finite resolution of experimental conditions, that is, finite angular and velocity

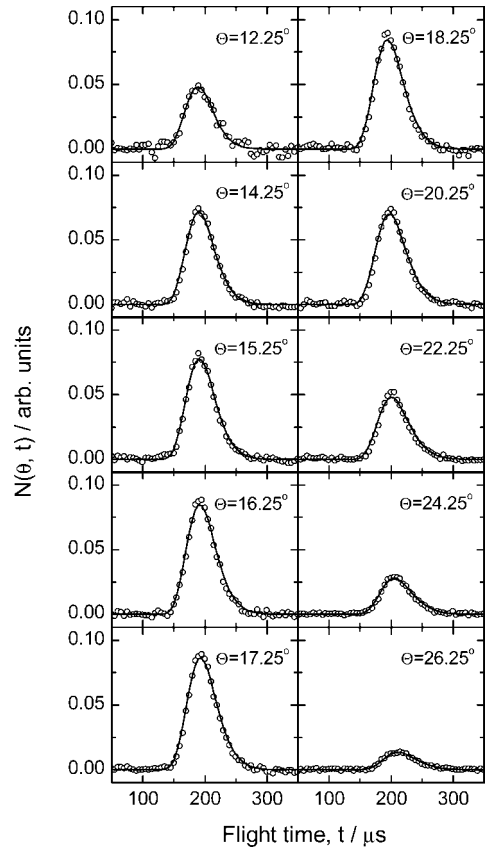

Figure 3. TOF distributions of the HCCS product (open circles) for the reaction S(^{1}D) + C_2H_2 at $E_c = 35.6$ kJ mol^{-1} at the indicated LAB angles. Solid lines represent the TOF distributions calculated from the best-fit CM functions reported in Figure 4.

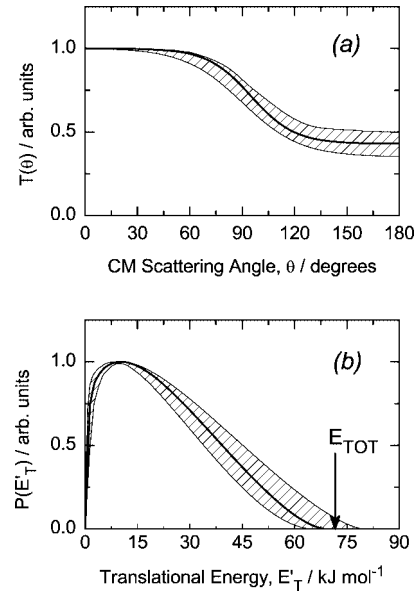

Figure 4. Best-fit CM product (a) angular and (b) translational energy distributions. The arrow in panel b indicates the total energy available to the products.

spread of the reactant beams and angular resolution of the detector, the LAB-CM transformation is not single-valued and, therefore, analysis of the laboratory data is carried out by the usual forward convolution procedure,[17] that is, the product CM angular, $T(\theta)$, and translational energy, $P(E'_T)$, distributions are assumed, averaged, and transformed to the LAB frame for comparison with the experimental data. The solid lines in

Figures 1 and 3 represent the curves calculated with the best fit functions depicted in Figure 4. The hatched areas in Figure 4 delimit the range of CM functions which still afford an acceptable fit of the data, that is, they represent the error bars of the present determination. The best CM angular distribution (Figure 4a) exhibits a significant intensity in the whole angular range, with a marked preference for the forward hemisphere with a best-fit ratio $T(180°)/T(0°)$ of 0.43. This ratio can vary by about ±0.10 within the error bar. Such a shape is consistent either with the competition of two reaction mechanisms (a direct one generating forward scattering and an indirect one generating a backward-forward symmetric angular distribution) or with the formation of a bound intermediate with a lifetime τ comparable to its rotational period τ_R (osculating model of chemical reaction).[50] If the latter is the case, from the difference of the intensity at the two poles it is possible to give an estimate of the complex lifetime[50] by means of the equation $T(180°)/T(0°) = e^{-\tau_R/2\tau}$, where $T(0°)$ and $T(180°)$ are the values assumed by $T(\theta)$ at the two poles. With the observed asymmetry of the CM angular distribution, the ratio τ/τ_R would be 0.6. A high degree of product rotational excitation is expected, due the specific mass combination of this reaction, on the basis of angular momentum conservation arguments and is witnessed by the lack of polarization of the CM angular distribution.

As far as the best-fit $P(E'_T)$ is concerned (Figure 4b), we note that the peak position is at about 7 kJ mol^{-1}, that is, quite close to $E'_T = 0$, which indicates the absence of a potential energy exit barrier. The fit of both angular and TOF distributions was very sensitive to the rise and the peak position, while it was less sensitive to the tail of the $P(E'_T)$, as clearly visible from the shape of the hatched area. The average product translational energy, defined as $\langle E'_T \rangle = \sum P(E'_T)E'_T/\sum P(E'_T)$ is about 23 kJ mol^{-1} corresponding to a fraction, f_T, of the total available energy ($E_{tot} = E_c - \Delta H^\circ_0$) of 0.32 using the theoretical value of $\Delta H^\circ_0 = -36.0$ kJ mol^{-1} for reaction 1.

5. Computational Results

The lowest stationary points localized along the PES of S(^{1}D) + C_2H_2 have been reported in Figure 5, where the main geometrical parameters (Ångstroms and degrees) are shown together with the energies computed at the B3LYP/aug-cc-pV(T+*d*)Z, CCSD(T)/ aug-cc-pV(T+*d*)Z and W1 levels, relative to that of thioketene (H_2CCS **1**) which is the most stable isomer at all levels of calculation. The enthalpy changes and barrier heights computed at 0 K with inclusion of the zero-point energy correction for the main isomerization and dissociation processes are reported in Table 1, while a schematic representation of the potential energy surface of the system S(^{1}D) + C_2H_2 is shown in Figure 6. For the sake of simplicity in Figure 6 we have reported only the relative energies computed at the W1 level, while in Table 1 we have reported the values computed at all levels of calculation for comparison purposes. The total energies, the geometrical parameters, and the vibrational frequencies of all the stationary points (minima and saddle points) are provided as Supporting Information (Table S1). For comparison purposes we report in Table 1 also the reaction enthalpy for S(^{3}P) + C_2H_2 → HCCS + H which was investigated recently by Woon using very accurate methods.[33] Our values are in very good agreement with the values computed by Woon at a comparable level of calculation: 62.1 kJ mol^{-1} with respect to 61.3 kJ mol^{-1} and 85.1 kJ mol^{-1} with respect to 84.8 kJ mol^{-1}, which is the best estimate of Woon. Many of the stationary points that are of interest in this work have been previously reported by Kaiser, Yamada, and Osamura in their

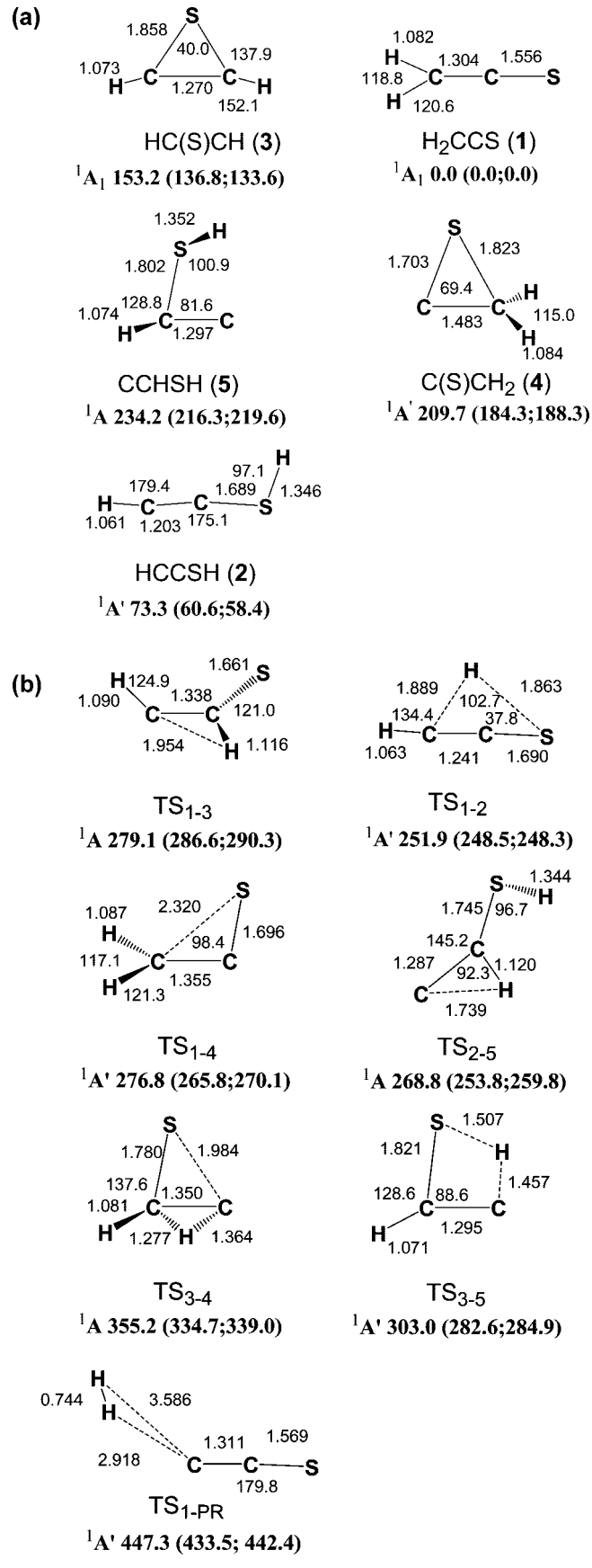

Figure 5. B3LYP optimized geometries (Ångstroms and degrees) and relative energies (kJ mol^{-1}) at 0 K (a) minima and (b) saddle points localized on the PES of S(^{1}D) + C_2H_2; CCSD(T) and W1 relative energies are reported in parentheses.

TABLE 1: Enthalpy Changes and Barrier Heights (kJ mol^{-1}, 0 K) Computed at the B3LYP/aug-cc-pV(T+*d*)Z, CCSD(T)/aug-cc-pV(T+*d*)Z and W1 Levels of Theory for Selected Dissociation and Isomerization Processes for the System S(^{1}D) + C_2H_2

	ΔH_0°			barrier height		
	B3LYP	CCSD(T)	W1	B3LYP	CCSD(T)	W1
HC(S)CH → S(^{1}D) + C_2H_2	266.5	266.1	280.7			
HC(S)CH → HC(S)C + H	350.6	355.2	365.0			
HC(S)CH → H_2CCS	−153.2	−136.8	−133.6	125.9	149.8	156.7
HC(S)CH → $C(S)CH_2$	56.5	47.5	54.7	202.0	197.9	205.4
HC(S)CH → CCHSH	81.0	79.5	86.0	149.8	145.8	151.3
$C(S)CH_2$ → H_2CCS	−209.7	−184.3	−188.3	67.1	81.5	81.8
H_2CCS → HCCS + H	371.2	377.8	378.3			
S(^{3}P) + C_2H_2 → HCCS + H	62.1	85.1	74.5			
H_2CCS → CCS ($^1\Delta$) + H_2	445.2	433.0	441.6	447.3	433.5	442.4
H_2CCS → CCS ($^3\Sigma^-$) + H_2	361.5	376.1	384.1			
H_2CCS → CS + CH_2 ($^1A_1$)	525.0	491.8	507.2			
H_2CCS → CS + CH_2 ($^3B_1$)	479.3	452.6	468.6			
H_2CCS → HCCSH	73.3	60.6	58.4	251.9	248.5	248.3
CCHSH → HCCSH	−160.9	−155.7	−161.2	34.6	37.5	40.2
CCHSH → CCH + SH	275.8	280.9	281.5			
HCCSH → HCCS + H	297.9	317.2	319.9			
HCCSH → CCSH + H	492.4	508.0	518.3			

study of the reaction C_2 + H_2S.[6,14] They optimized the geometries at the B3LYP/6-311G(d,p) level and computed the energies at the CCSD(T)/aug-cc-pVTZ level. The agreement between our work and their results is good both at the B3LYP and CCSD(T) levels, the differences being due to the larger basis set used in this work. The reaction C_2 + H_2S was recently studied also by Wang et al.[51] Also in this case the agreement of our results with respect to their B3LYP optimized geometries is good, while small differences are present with respect to their MP2 and QCISD optimized geometries, as expected.

In the following paragraph we will discuss our results; for simplicity we will refer only to the most accurate results, that is, the W1 results. The B3LYP and CCSD(T) values however are reported in Figure 5 and Table 1. As shown in Figure 6, the interaction of S(^{1}D) with C_2H_2 gives rise without any barrier to the cyclic species HC(S)CH (**3**), which is more stable than the reactants by 280.7 kJ mol^{-1} at the W1 level. Species **3** can isomerize to H_2CCS (**1**), *c*-$C(S)CH_2$ (**4**), and CCHSH (**5**) with barriers of 156.7, 205.4, 151.3 kJ mol^{-1}, respectively. However, only the first isomerization leads to a more stable species. Finally, the species HC(S)CH (**3**) can undergo a C−H bond fission and produce the cyclic-C(S)CH isomer plus H. Once formed, species **4** can isomerize to species **1** with a relatively low barrier (81.8 kJ mol^{-1}), while species **5** gives HCCSH (**2**) with a barrier as low as 40.2 kJ mol^{-1}. Species **2** can be formed also from **1** but the barrier for this endothermic isomerization is quite high (248.3 kJ mol^{-1}). Species **2** can lose one H giving rise to HCCS (+319.9 kJ mol^{-1}) or CCSH (+518.3 kJ mol^{-1}). H_2CCS can dissociate into HCCS + H or into H_2 and CCS ($^1\Delta$). This last pathway is endothermic by 441.6 kJ mol^{-1} at the W1 level and shows also a very late transition state. The geometry of this saddle point, reported in Figure 5, shows that

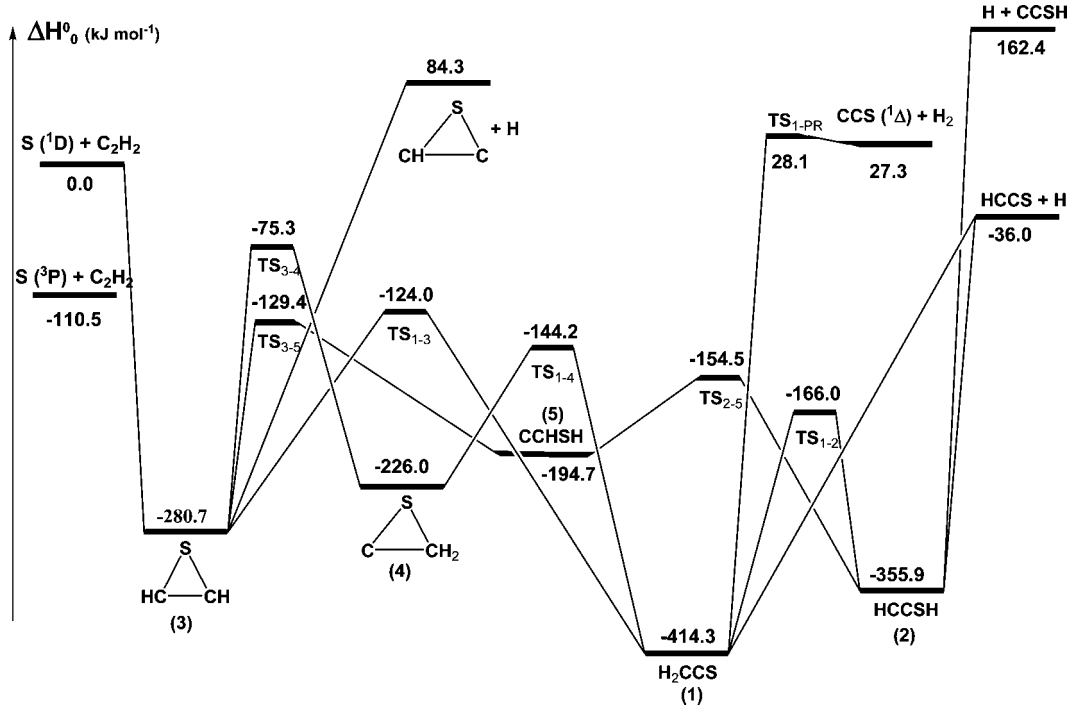

Figure 6. Schematic representation of the S(^{1}D) + C_2H_2 potential energy surface. For simplicity, only the W1 relative energies (kJ mol^{-1}) are reported.

the H_2 molecule is already formed and the interaction with CCS is almost absent. As a result, the imaginary frequency of this saddle is very small, only 23.1 cm^{-1}, and the barrier height with respect to the products is very low (0.8 kJ mol^{-1}).

We have also explored the possibility that $S(^1D)$ directly inserts into one of the CH bonds of acetylene. Quite interestingly, we could not locate a transition state for $S(^1D)$ insertion, so that direct insertion is also a barrierless process. However, we have verified that the system evolves toward addition rather than insertion for most of the possible attack geometries. Even an approaching S−H−C angle of 174° leads the sulfur atom toward the π-orbitals of acetylene, while larger S−H−C angles do not evolve into a reactive collision. In conclusion, $S(^1D)$ insertion does not appear to be a competitive reaction mechanism in the presence of π-bonds, as already noted for other reactions involving unsaturated hydrocarbons and insertive species.[52]

6. Discussion on the Reaction Mechanism

The reactive scattering results clearly indicate that a product of general formula C_2HS is formed through a S/H exchange channel and that the reaction pathway leading to C_2HS proceeds through the formation of a bound intermediate of general formula C_2H_2S. In the assumption that the forward scattering preference is associated with the osculating complex mechanism, the lifetime of the bound intermediate is comparable to its rotational period. This is what one would expect from the features of the singlet C_2H_2S PES derived in the present work (Figure 6). As a matter of fact, there are two possible pathways leading to the only exothermic H-displacement channel and both of them are affected by the formation of bound intermediates. In both cases, the first step is the electrophilic addition of $S(^1D)$ to the π-system of acetylene, leading to a first addition cyclic intermediate (thiirene). Once formed, thiirene can directly rearrange by ring opening and H migration to H_2CCS (thioketene, the most stable isomer along the singlet C_2H_2S PES) through a barrier of 156.7 kJ mol^{-1}. Once formed, thioketene can dissociate directly to HCCS + H or $CCS(^1\Delta) + H_2$. The latter channel, barely accessible at the collision energy of the present experiment, has not been observed. In the alternative pathway, the PES minimum configuration of thioketene is never reached and the succession of rearrangements after thiirene formation is isomerization to CCHSH (through a barrier of 151.3 kJ mol^{-1}) followed by isomerization to HCCSH (through a barrier of 40.2 kJ mol^{-1}), which in turn can undergo an S−H bond fission to HCCS + H. There are no simple arguments to infer which of the two pathways is the dominant one; the isomerization from thiirene to thioketene is characterized by a larger isomerization barrier, but in the second pathway it is necessary to undergo two isomerizations before reaching the configuration of an intermediate, HCCSH, which can dissociate into HCCS + H products. RRKM estimates could help to elucidate which of the two pathways is the dominant one. Preliminary estimates[53] indicate that the rate constant associated to isomerization from thiirene to thioketene, $k_{3\rightarrow1} = 8 \times 10^9$ s^{-1}, is smaller than the one associated to the isomerization to CCHSH, $k_{3\rightarrow5} = 2 \times 10^{10}$ s^{-1}. The conversion from CCHSH to HCCSH is also very fast with $k_{5\rightarrow2} = 7 \times 10^{10}$ s^{-1}. There is also a third pathway, which proceeds through the rearrangement into *c*-$C(S)CH_2$, through the largest isomerization barrier from thiirene, +205.4 kJ mol^{-1}, followed by an isomerization to H_2CCS. This last possibility appears to be less favored because of the large isomerization barrier and the need of two rearrangement steps. Because of the large isomerization barrier, according to preliminary RRKM calculations $k_{3\rightarrow4} = 5 \times 10^8$ s^{-1}.

As for the molecular hydrogen elimination channel, the lack of $C_2S(^1\Delta)$ observation is not surprising, because at the collision energy of the present experiment, channel 4 has just become open on energetic grounds, but the rise of the reactive excitation function to appreciable values can be quite displaced from its onset. The failure to observe the C_2S ($^3\Sigma^-$) product implies that ISC from the singlet to the triplet PES and the subsequent reaction along it are not occurring to an appreciable extent under the conditions of our experiment. Of course, we cannot rule out that ISC occurs at all, especially because the presence of a sulfur atom with a relatively large atomic weight may make the spin conservation rule less rigid, as demonstrated in recent studies of the reactions $S(^1D)+H_2$[54]and S+SH[55] and of the high temperature pyrolysis of H_2S.[56] Since we did not observe C_2S ($^3\Sigma^-$) formation and we could not see any features of ISC to the triplet PES for the H-displacement channel, we can conclude that if ISC occurs, the most probable outcome is quenching to $S(^3P)+C_2H_2$.

It is quite interesting to compare the reaction dynamics of the title reaction, as derived from the present experimental and theoretical results, to that of the related reaction $C_2(X\ ^1\Sigma^+_g) + H_2S$ recently investigated by Kaiser et al.[14] The two reactions, in fact, experience the same singlet C_2H_2S PES with the reactant asymptote higher in energy by 196 kJ mol^{-1} in the case of the reaction $C_2 + H_2S$. Kaiser et al.[14] have identified HCCS+H as the main reaction channel in their crossed beam experiment, while an attempt to identify the H_2 elimination channel was inconclusive because of the poor signal-to-noise ratio at m/z = 56. Nevertheless, a difference was noted in the fast part of the m/z = 57 and 56 TOF spectra, which could be taken as an indication that the H_2 elimination channel is open in the $C_2(X\ ^1\Sigma^+_g) + H_2S$ reaction. In that case, there are three possible exothermic H_2 elimination channels of which two are associated to the formation of singlet SC_2 isomers (that is cyclic-$SC_2(^1A_1)$ and linear $SC_2(^1\Delta)$) and one to the ground state $^3\Sigma^-$ of SC_2. Since the CM functions could not be extracted from those experimental results, it is unclear whether the H_2 elimination channel proceeded through ISC to the triplet PES. The HCCS+H channel, instead, was inferred to be produced from a S−H bond fission of HSCCH or a C−H bond fission of H_2CCS, exactly as in the present study of the $S(^1D) + C_2H_2$ reaction. One important difference is that in the C_2+H_2S case both HSCCH and H_2CCS could only be formed after extensive rearrangement of the initial addition intermediate H_2SCC. Also, the total available energy to the bound intermediates is much higher, which is reflected in the much more pronounced forward bias of the derived CM angular distribution pointing to much shorter intermediate lifetimes. The $P(E'_T)$s for the two systems show some similarities in their shape (once scaled for the total available energy of the two cases) which might suggest that the two reactions experience the same exit channel PES features.

Finally, it is also quite interesting to compare the present results with those of the related reactions involving the same substrate acetylene and other atomic species. Probably the two reactions most strongly related are those involving the electronically excited states of atomic nitrogen and carbon:

$$N(^2D)+C_2H_2 \rightarrow \text{products} \quad (8)$$

$$C(^1D)+C_2H_2 \rightarrow \text{products} \quad (9)$$

both studied in crossed beam experiments.[18,20,21,57] In both cases, the first step of the reaction is the addition of the $N(^2D)$ and

C(^{1}D) to the π-system of acetylene with formation of the cyclic intermediates *c*-HC(N)CH and *c*-C_3H_2, in all respects equivalent to thiirene. Both *c*-HC(N)CH and *c*-C_3H_2 addition intermediates can dissociate directly to cyclic-HC(N)C + H and cyclic-C_3H + H, since these reactive channels are energetically open in those cases, in contrast to the title reaction, where the formation of *c*-HC(S)C(^{2}A″) + H(^{2}S) is strongly endothermic. In those systems as well, the addition cyclic intermediates can isomerize in one step (reaction 9) or two steps (reaction 8) to a species equivalent to H_2CCS, that is H_2CCC and H_2CCN in the two cases. In the case of reaction 8, H_2CCN is the global minimum of the C_2H_2N PES, while in the case of reaction 9 *c*-C_3H_2 is actually the global minimum of the related PES. Finally, in both cases as well as in the case of the title reaction, the formation of another intermediate similar to HCCSH, that is, HCCNH and HCCCH, is amenable. The situation of the C_2H_2N system is the most similar to that of the title reaction as far as the relative position of the intermediates along the minimum energy path is concerned. Interestingly, in that case it was shown by RRKM calculations that the reaction mainly proceeded through the cyclic and HCCNH intermediates with the global minimum configuration of H_2CCN never experienced by the system.[18]

7. The HCCS Electron Ionization Efficiency Curve

The capability of tuning the ionizing electron energy has also permitted us to obtain information on the ionization energy of the thioketenyl (HCCS) radical product, a quantity for which to our knowledge no experimental data currently exist. There is some interest in the HCCS(X $^2\Pi$) radical, the smallest member in the $HC_{n+1}S$ series of molecules that are important intermediates in combustion[1] and interstellar chemistry.[2,3] It has been investigated extensively both experimentally and theoretically. In particular, much work has focused on its electronic[58] and rotational spectroscopy.[59] These studies have provided spectroscopic constants, excitation energy and some of the vibrational frequencies of the ground and first excited states. The Renner−Teller effect in this linear radical has also been investigated.[58,60] Ab initio electronic structure calculations at the coupled-cluster level of theory have confirmed that ground-state HCCS has a linear structure.[59] Very recently the HCCS radical and its related cation, $HCCS^+$, and anion, $HCCS^-$, have been investigated at a high level of accuracy by Puzzarini.[61] A systematic study of their equilibrium structure and dipole moment was carried out at the coupled-cluster level of theory in conjunction with correlation consistent basis sets ranging in size from quadruple to sextuple zeta. Extrapolation to the complete basis set limit and additional corrections due to core-valence correlation were also considered. The computed energies were employed for evaluating the ionization potential and the electron affinity. The linear $HCCS^+$ species ($X^3\Sigma^-$) has been found to be the ground state, but the lowest singlet electronic state ($A^1\Sigma^+$) has also been investigated. From the computed energies, the equilibrium adiabatic ionization energy IE of HCCS [$IE_{ad} = E(HCCS^+) - E(HCCS)$] was given for both triplet and singlet states of $HCCS^+$. The zero-point corrected values are 9.114 and 9.958 eV, respectively. We have also computed the ionization energy of HCCS. Our values for the adiabatic IE are 9.08 eV (10.14 eV) at B3LYP/aug-cc-pV(T+*d*)Z level, 9.08 eV (9.96 eV) at CCSD(T)/aug-cc-pV(T+*d*)Z level and 9.17 eV (10.08 eV) at W1 level with inclusion of ZPE correction in all calculations, for the triplet (singlet) state of $HCCS^+$. The vertical IEs are computed by us to be 9.15 eV both at B3LYP/aug-cc-pV(T+*d*)Z level and at CCSD(T)/aug-cc-pV(T+*d*)Z level. The adiabatic values compare very well with the extremely accurate value recently computed by Puzzarini of 9.114 eV.[60]

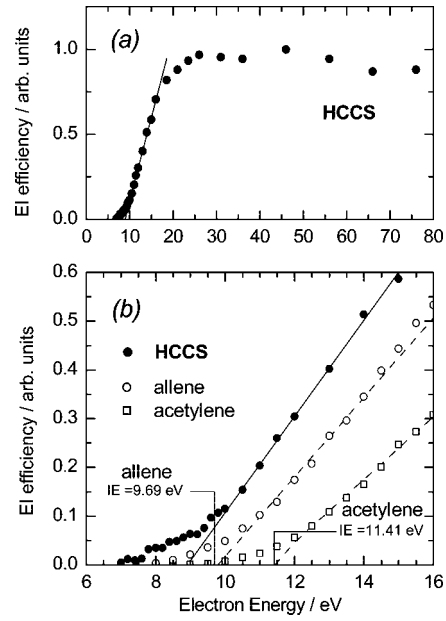

Figure 7. (a) Electron ionization efficiency as a function of electron energy of the HCCS radical product ($m/z = 57$) from the S(^{1}D) + C_2H_2 reaction at $E_c = 35.6$ kJ mol^{-1}, measured at the CM angle, compared in the enlargement (b) to those of allene (C_3H_4, $m/z = 40$) and acetylene (C_2H_2, $m/z = 26$) contained in a supersonic beam of the pure species. The literature IE values of allene and acetylene are indicated. The estimated ionization threshold of the "hot" HCCS reaction product is 8.9 ± 0.3 eV (see text).

The experimental electron ionization efficiency curve (i.e., the ionization cross section as a function of electron energy) of the HCCS product was measured by detecting the $m/z = 57$ signal intensity at the CM angle as a function of electron energy from threshold up to 80 eV. The entire efficiency curve is shown in Figure 7a, while Figure 7b depicts an expanded view (from threshold up to 16 eV) of the efficiency curve of HCCS. Figure 7b also reports the efficiency curves for acetylene and allene, both produced in supersonic beams of the pure species, where they are expected to be vibrationally and also rotationally cold. Since the IE for the two species are known, they are here used to calibrate the absolute electron energy scale. After calibration, the ionization threshold of HCCS was determined to be 8.9 ± 0.3 eV from the simple straight-line extrapolation method, also used to calibrate the energy scale. We note that this value, which is a vertical ionization energy, is about 0.2 eV lower than the calculated IE. However, it should be noted that the probed HCCS radical is formed by the S(^{1}D) + C_2H_2 reaction at a collision energy of 35.6 kJ mol^{-1} and therefore contains a certain amount of internal energy. From the experimentally determined fraction of energy released as product translational energy, we can derive the complementary value for the average ro-vibrational energy content of HCCS, which is 46 kJ mol^{-1} (0.48 eV). The question then arises whether, and eventually to what extent, the internal excitation of the radical has an influence on its observed ionization threshold. Interestingly in this regard, recent work by Cool et al.[62] based on measurements by tunable VUV synchrotron radiation of photoionization efficiency curves of a variety of hydrocarbon molecules and radicals produced in flames, has found that the apparent ionization thresholds of those species closely match their accepted ionization energies. In the present case, there is not an experimentally accepted IE value for HCCS; however, we do have accurate theoretical results for it. It should be noted that while under our experimental condition there is no relaxation of the internal degrees

of freedom of the detected radical formed from the chemical reaction, in the flame experiments significant vibrational relaxation can occur during the gas dynamic expansion of the molecules sampled by the quartz cone from a region at 20−40 torr. Therefore, in our case the experimentally determined ionization threshold may reasonably be expected to be somewhat red shifted with respect to that of internally cold HCCS. Indeed, ca. 0.5 eV of average internal energy of the HCCS radical seems to determine a red shift of about 0.2 eV in the electron ionization efficiency curve threshold with respect to accurate theoretical values. Considering some uncertainty in our determination (relative to acetylene and allene), this shift may be smaller than 0.2 eV, and therefore there appears to be an overall good agreement between experiment and theory. In conclusion, the theoretical IE of HCCS of 9.11 eV, with an accuracy of 0.05 eV,[61] can be considered reliably as the true IE of ground-state HCCS.

8. Conclusion

The reaction dynamics of excited sulfur atoms, $S(^1D)$, with acetylene has been investigated by the crossed beam scattering technique with mass spectrometric detection and TOF analysis at the collision energy of 35.6 kJ mol^{-1}. These studies have been made possible by the development of intense continuous supersonic beams of $S(^3P,^1D)$ atoms. From product angular and TOF distributions, center-of-mass product angular and translational energy distributions have been derived. The $S(^1D) + C_2H_2$ reaction is found to lead to formation of HCCS (thioketenyl) + H, while the only other energetically allowed channels, those leading to $CCS(^3\Sigma^-, {}^1\Delta) + H_2$, are not observed to occur to an appreciable extent. The HCCS product CM angular distribution indicates that the reaction proceeds through the formation of an osculating complex. The fraction of total available energy released into product translation is 0.32, which is a result that points to a considerable internal (ro-vibrational) excitation of the HCCS radical product. The interpretation of the scattering results and of the HCCS product ionization energy has benefitted from synergic high-level ab initio electronic structure calculations of stationary points and product energetics for the singlet C_2H_2S potential energy surface at the B3LYP and CCSD(T) levels of theory, with thermochemical calculations also performed at the W1 level. From this combined experimental and theoretical study we conclude that the $S(^1D) + C_2H_2$ reaction proceeds by addition of the excited sulfur atom to the triple bond of acetylene forming a stable thiirene intermediate that isomerizes either to the more stable singlet thioketene or in two steps to HCCSH. Once formed, the intermediates H_2CCS and HCCSH dissociate to HCCS + H because of their high internal energy content within a time comparable to their rotational periods. Measurements of the electron ionization efficiency curve, from 80 eV down to the ionization threshold, for the $m/z = 57$ product have allowed us to obtain an estimate (8.9 ± 0.3 eV) of the ionization energy of the thioketenyl radical produced by the chemical reaction. The adiabatic IE of HCCS is computed to be 9.08 eV both at the B3LYP/aug-cc-pV(T+*d*)Z and CCSD(T)/aug-cc-pV(T+*d*)Z levels and 9.17 eV at the W1 level with inclusion of ZPE correction in all calculations, while the vertical IE is computed to be 9.15 eV both at the B3LYP/aug-cc-pV(T+*d*)Z level and at the CCSD(T)/aug-cc-pV(T+*d*)Z level. These theoretical results indicate that the observed ionization energy of the internally, somewhat hot HCCS radical product is red shifted by about 0.2 eV with respect to that of ground-state HCCS.

These studies offer considerable promise for further crossed beam dynamical investigations of other sulfur atom reactions of particular relevance to combustion and atmospheric chemistry.

Acknowledgment. We acknowledge financial support from the Italian MIUR (Ministero Istruzione Università Ricerca) under Projects PRIN (2007H9S8SW_004 and 2007WLBXX9_004). This work has also been supported by the European Union Marie-Curie human resources and mobility programme, including a postdoctoral fellowship for K.M.H. under contract MCRTN-CT-2004-512302, Molecular Universe. W.D.G. gratefully acknowledges the Swedish Research Council for his Senior Researcher grant (Contract Number 2006-427). We thank Dimitris Skouteris for allowing us to use his RRKM calculations before publication.

Supporting Information Available: This material is available free of charge via the Internet at http://pubs.acs.org.

References and Notes

(1) (a) Petherbridge, J. R.; May, P. W.; Shallcross, D. E.; Harvey, J. N.; Fuge, G. M.; Rosser, K. N.; Ashfold, M. N. R. *Diamond Relat. Mater.* **2003**, *12*, 2178. (b) Petherbridge, J. R.; May, P. W.; Fuge, G. M.; Rosser, K. N.; Ashfold, M. N. R. *Diamond Relat. Mater.* **2002**, *11*, 301.

(2) (a) Morell, G.; Gonzalez-Berrýos, A.; Weiner, B. R.; Gupta, S. *J. Mater. Sci.: Mater. Electron.* **2006**, *17*, 443. (b) Haubner, R.; Sommer, D. *Diamond Relat. Mater.* **2003**, *12*, 298.

(3) Nishitani-Gamo, M.; Yasu, E.; Xiao, C. Y.; Kikuchi, Y.; Ushizawa, K.; Sakaguchi, I.; Suzuki, T.; Ando, T. *Diamond Relat. Mater.* **2000**, *9*, 941.

(4) Schofield, K. *Combust. Flame* **2001**, *124*, 137.

(5) Bates, T. S.; Lamb, B. K.; Guenther, A.; Dignon, J.; Stoiber, R. E. *J. Atmos. Chem.* **1992**, *14*, 315.

(6) Yamada, M.; Osamura, Y.; Kaiser, R. I. *Astron. Astrophys.* **2002**, *395*, 1031.

(7) Petrie, S. *Mon. Not. R. Astron. Soc.* **1996**, *281*, 666.

(8) Dello Russo, N.; DiSanti, M. A.; Mumma, M. J.; Magee-Sauer, K.; Rettig, T. W. *Icarus* **1998**, *135*, 377.

(9) See, for instance: Krasnopolsky, V. A. *Icarus* **2007**, *191*, 25.

(10) See, for instance: (a) Liu, K.; Han, W.; Pan, W.-P.; Riley, J. T. *J. Hazard. Mater.* **2001**, *B84*, 175. (b) Ristovski, Z. D.; Jayaratne, E. R.; Lim, M.; Ayoko, G. A.; Morawska, L. *Environ. Sci. Technol.* **2006**, *40*, 1314.

(11) Noll, K. S.; McGrath, M. A.; Trafton, L. M.; Atreya, S. K.; Caldwell, J. J.; Weaver, H. A.; Yelle, R. V.; Barnet, C. *Edgington Science* **1995**, *267*, 1307.

(12) Atreya, S. K.; Edginton, S. G.; Trafton, L. M.; Caldwell, J. J.; Noll, K. S.; Weaver, H. A. *Geophys. Res. Lett.* **1995**, *22*, 1625.

(13) Kaiser, R. I.; Ochsenfeld, C.; Head-Gordon, M.; Lee, Y. T. *Science* **1998**, *279*, 1181.

(14) Kaiser, R. I.; Yamada, M.; Osamura, Y. *J. Phys. Chem. A* **2002**, *106*, 4825.

(15) Sibener, S. J.; Buss, R. J.; Ng, C.-Y.; Lee, Y. T. *Rev. Sci. Instrum.* **1980**, *51*, 167.

(16) Alagia, M.; Aquilanti, V.; Ascenzi, D.; Balucani, N.; Cappelletti, D.; Cartechini, L.; Casavecchia, P.; Pirani, F.; Sanchini, G.; Volpi, G. G. *Israel J. Chem.* **1997**, *37*, 329.

(17) Alagia, M.; Balucani, N.; Casavecchia, P.; Stranges, D.; Volpi, G. G. *J. Chem. Soc., Faraday Trans.* **1995**, *91*, 575.

(18) Balucani, N.; Alagia, M.; Cartechini, L.; Casavecchia, P.; Volpi, G. G.; Sato, K.; Takayanagi, T.; Kurosaki, Y. *J. Am. Chem. Soc.* **2000**, *122*, 4443.

(19) (a) Alagia, M.; Balucani, N.; Cartechini, L.; Casavecchia, P.; van Beek, M.; Volpi, G. G.; Bonnet, L.; Rayez, J.-C. *Faraday Discuss.* **1999**, *113*, 133. (b) Alagia, M.; Balucani, N.; Casavecchia, P.; Laganà, A.; Ochoa de Aspuru, G.; van Kleef, E. H.; Volpi, G. G.; Lendvay, G. *Chem. Phys. Lett.* **1996**, *258*, 323. (c) Balucani, N.; Stranges, D.; Casavecchia, P.; Volpi, G. G. *J. Chem. Phys.* **2004**, *120*, 9571.

(20) (a) Costes, M.; Daugey, N.; Naulin, C.; Bergeat, A.; Leonori, F.; Segoloni, E.; Petrucci, R.; Balucani, N.; Casavecchia, P. *Faraday Discuss.* **2006**, *133*, 157. (b) Leonori, F.; Petrucci, R.; Segoloni, E.; Bergeat, A.; Hickson, K. M.; Balucani, N.; Casavecchia, P. *J. Phys. Chem. A* **2008**, *112*, 1363.

(21) (a) Leonori, F.; Petrucci, R.; Hickson, K. M.; Segoloni, E.; Balucani, N.; Le Picard, S.; Foggi, P.; Casavecchia, P. *Planet. Space Sci.* **2008**, *56*, 1658. (b) Balucani, N.; Leonori, F.; Petrucci, R.; Hickson, K. M.; Casavecchia, P. *Phys. Scr.* **2008**, *78*, 058117.

(22) (a) Balucani, N.; Casavecchia, P.; Aoiz, F. J.; Bañares, L.; Castillo, J. F.; Herrero, V. J. *Mol. Phys.* **2005**, *103*, 1703. (b) Alagia, M.; Balucani, N.; Casavecchia, P.; Volpi, G. G. *J. Phys. Chem. A* **1997**, *101*, 6455. (c) Balucani, N.; Beneventi, L.; Casavecchia, P.; Volpi, G. G.; Kruus, E. J.; Sloan, J. J. *Can. J. Chem.* **1994**, *72*, 888.

(23) (a) Bergeat, A.; Cartechini, L.; Balucani, N.; Capozza, G.; Phillips, L. F.; Casavecchia, P.; Volpi, G. G.; Bonnet, L.; Rayez, J.-C. *Chem. Phys. Lett.* **2000**, *327*, 197. (b) Balucani, N.; Capozza, G.; Cartechini, L.; Bergeat, A.; Bobbenkamp, R.; Casavecchia, P.; Aoiz, F. J.; Bañares, L.; Honvault, P.; Bussery-Honvault, B.; Launay, J.-M. *Phys. Chem. Chem. Phys.* **2004**, *6*, 4957. (c) Balucani, N.; Capozza, G.; Segoloni, E.; Russo, A.; Bobbenkamp, R.; Casavecchia, P.; Gonzalez-Lezana, T.; Rackham, E. J.; Bañares, L.; Aoiz, F. J. *J. Chem. Phys.* **2005**, *122*, 234309.

(24) Leonori, F.; Petrucci, R.; Balucani, N.; Casavecchia, P.; Rosi, M.; Skouteris, D. Università degli Studi di Perugia, Perugia, Italy. Unpublished work, 2009.

(25) (a) Lee, S.-H.; Liu, K. *Chem. Phys. Lett.* **1998**, *290*, 323. (b) Lee, S.-H.; Liu, K. *Appl. Phys. B* **2000**, *71*, 627.

(26) Khachatrian, A.; Dagdigian, P. J. *J. Chem. Phys.* **2005**, *122*, 024303.

(27) Khachatrian, A.; Dagdigian, P. J. *Chem. Phys. Lett.* **2005**, *402*, 265.

(28) Halmer, M. M.; Schmincke, H.-U.; Graf, H.-F. *J. Volcanol. Geotherm. Res.* **2002**, *115*, 511.

(29) See, for instance: (a) Kim, M. H.; Li, W.; Lee, S. K.; Suits, A. G. *Can. J. Chem.* **2004**, *82*, 880.

(30) Cook, P. A.; Langford, S. R.; Dixon, R. N.; Ashfold, M. N. R. *J. Chem. Phys.* **2001**, *114*, 1672.

(31) Schofield, K. *J. Phys. Chem. Ref. Data* **1979**, *8*, 723.

(32) Black, G.; Jusinski, L. E. *J. Chem. Phys.* **1985**, *82*, 789.

(33) Woon, D. E. *J. Phys. Chem. A* **2007**, *111*, 11249.

(34) Little, D. J.; Donovan, R. J. *J. Photochem.* **1972**, *1*, 371.

(35) Van Roodselaar, A.; Safarik, I.; Strausz, O. P.; Gunning, H. E. *J. Am. Chem. Soc.* **1978**, *100*, 4068.

(36) (a) Casavecchia, P.; Capozza, G.; Segoloni, E.; Leonori, F.; Balucani, N.; Volpi, G. G. *J. Phys. Chem. A* **2005**, *109*, 3527. (b) Capozza, G.; Segoloni, E.; Leonori, F.; Volpi, G. G.; Casavecchia, P. *J. Chem. Phys.* **2004**, *120*, 4557.

(37) Casavecchia, P.; Leonori, F.; Balucani, N.; Petrucci, R.; Capozza, G.; Segoloni, E. *Phys. Chem. Chem. Phys.* **2009**, *11*, 46.

(38) Balucani, N.; Capozza, G.; Leonori, F.; Segoloni, E.; Casavecchia, P. *Int. Rev. Phys. Chem.* **2006**, *25*, 109.

(39) Leonori, F.; Petrucci, R.; Balucani, N.; Casavecchia, P., Rosi, M.; Le Picard, S.; Canosa, A.; Sims, I. R. *Phys. Chem. Chem. Phys.*, in press (first published as an Advance Article on the web February 3, 2009; DOI: 10.1039/b9000059c).

(40) Leonori, F.; Petrucci, R.; Wang, X.; Balucani, N.; Casavecchia, P.; Rosi, M. Università degli Studi di Perugia, Perugia, Italy. Unpublished work, 2009.

(41) (a) Becke, A. D. *J. Phys. Chem.* **1993**, *98*, 5648. (b) Stephens, P. J.; Devlin, F. J.; Chablowski, C. F.; Frisch, M. J. *J. Phys. Chem.* **1994**, *98*, 11623.

(42) (a) Dunning, T. H., Jr. *J. Chem. Phys.* **1989**, *90*, 1007. (b) Woon, D. E.; Dunning, T. H., Jr. *J. Chem. Phys.* **1993**, *98*, 1358. (c) Kendall, R. A.; Dunning, T. H., Jr.; Harrison, R. J. *J. Chem. Phys.* **1992**, *96*, 6796.

(43) Bauschlicher, C. W., Jr.; Partridge, H. *Chem. Phys. Lett.* **1995**, *240*, 533.

(44) Martin, J. M. L.; Uzan, O. *Chem. Phys. Lett.* **1998**, *282*, 16.

(45) (a) Bartlett, R. J. *Annu. Rev. Phys. Chem.* **1981**, *32*, 359. (b) Raghavachari, K.; Trucks, G. W.; Pople, J. A.; Head-Gordon, M. *Chem. Phys. Lett.* **1989**, *157*, 479. (c) Olsen, J.; Jorgensen, P.; Koch, H.; Balkova, A.; Bartlett, R. J. *J. Chem. Phys.* **1996**, *104*, 8007.

(46) Shiina, H.; Miyoshi, A.; Matsui, H. *J. Phys. Chem. A* **1998**, *102*, 3556.

(47) (a) Martin, J. M. L.; de Oliveira, G. *J. Chem. Phys.* **1999**, *111*, 1843. (b) Parthiban, S.; Martin, J. M. L. *J. Chem. Phys.* **2001**, *114*, 6014.

(48) Frisch, M. J.; Trucks, G. W.; Schlegel, H. B.; Scuseria, G. E.; Robb, M. A.; Cheeseman, J. R.; Montgomery, J. A., Jr.; Vreven, T.; Kudin, K. N.; Burant, J. C.; Millam, J. M.; Iyengar, S. S.; Tomasi, J.; Barone, V.; Mennucci, B.; Cossi, M.; Scalmani, G.; Rega, N.; Petersson, G. A.; Nakatsuji, H.; Hada, M.; Ehara, M.; Toyota, K.; Fukuda, R.; Hasegawa, J.; Ishida, M.; Nakajima, T.; Honda, Y.; Kitao, O.; Nakai, H.; Klene, M.; Li, X.; Knox, J. E.; Hratchian, H. P.; Cross, J. B.; Bakken, V.; Adamo, C.; Jaramillo, J.; Gomperts, R.; Stratmann, R. E.; Yazyev, O.; Austin, A. J.; Cammi, R.; Pomelli, C.; Ochterski, J. W.; Ayala, P. Y.; Morokuma, K.; Voth, G. A.; Salvador, P.; Dannenberg, J. J.; Zakrzewski, V. G.; Dapprich, S.; Daniels, A. D.; Strain, M. C.; Farkas, O.; Malick, D. K.; Rabuck, A. D.; Raghavachari, K.; Foresman, J. B.; Ortiz, J. V.; Cui, Q.; Baboul, A. G.; Clifford, S.; Cioslowski, J.; Stefanov, B. B.; Liu, G.; Liashenko, A.; Piskorz, P.; Komaromi, I.; Martin, R. L.; Fox, D. J.; Keith, T.; Al-Laham, M. A.; Peng, C. Y.; Nanayakkara, A.; Challacombe, M.; Gill, P. M. W.; Johnson, B.; Chen, W.; Wong, M. W.; Gonzalez, C.; Pople, J. A. *Gaussian 03*, revision D.01; Gaussian, Inc.: Wallingford, CT, 2004.

(49) (a) Flükiger, P.; Lüthi, H. P.; Portmann, S.; Weber, J. *MOLEKEL 4.3*; Swiss Center for Scientific Computing: Manno, Switzerland, 2000−2002. (b) Portmann, S.; Lüthi, H. P. *Chimia* **2000**, *54*, 766.

(50) (a) Fisk, G. A.; Mc Donald, J. D.; Herschbach, D. R. *Discuss. Faraday Soc.* **1967**, *44*, 228. (b) Miller, W. B.; Safron, S. A.; Herschbach, D. R. *Discuss. Faraday Soc.* **1967**, *44*, 108. (c) Miller, W. B.; Safron, S. A.; Herschbach, D. R. *J. Chem. Phys.* **1972**, *56*, 3581.

(51) Wang, J.-H.; Han, K.-L.; He, G.-Z.; Li, Z. *Chem. Phys. Lett.* **2003**, *368*, 139.

(52) (a) Thiesemann, H.; Clifford, E. P.; Taatjes, C. A.; Klippenstein, S. J. *J. Phys. Chem. A* **2001**, *105*, 5393. (b) Nguyen, T. L.; Mebel, A. M.; Lin, S. H.; Kaiser, R. I. *J. Phys. Chem. A* **2001**, *105*, 11549.

(53) Skouteris, D., unpublished results, Università deg li Studi di Perugia, 2008. Estimates made by using the W1 results and considering the experimental collision energy and a reaction total angular momentum maximum of 50.

(54) Maiti, B.; Schatz, G. C.; Lendvay, G. *J. Phys. Chem. A* **2004**, *108*, 8772.

(55) Zhou, C.; Sendt, K.; Haynes, B. S. *J. Phys. Chem. A* **2008**, *112* (14), 3239.

(56) (a) Woiki, D.; Roth, P. *J. Phys. Chem.* **1994**, *98*, 12958. (b) Shiina, H.; Oya, M.; Yamashita, K.; Miyoshi, A.; Matsui, H. *J. Phys. Chem.* **1996**, *100*, 2136.

(57) Kaiser, R. I.; Mebel, A. M.; Lee, Y. T. *J. Chem. Phys.* **2001**, *114*, 231.

(58) Dunlop, J. R.; Karolczak, J.; Clouthier, D. J. *Chem. Phys. Lett.* **1988**, *151*, 362.

(59) Kohguchi, H.; Ohshima, Y.; Endo, Y. *Chem. Phys. Lett.* **1996**, *254*, 397.

(60) Flores, J. R. *J. Phys. Chem. B* **2003**, *107*, 9711, and references therein.

(61) Puzzarini, C. *Chem. Phys.* **2008**, *346*, 45.

(62) Cool, T. A.; Nakajima, K.; Mostefaoui, T. A.; Qi, F.; McIlroy, A.; Westmoreland, P. R.; Law, M. E.; Poisson, L.; Peterska, D. S.; Ahmed, M. *J. Chem. Phys.* **2003**, *119*, 8356.

JP810989P